A Modified Perturbation Method for Solving Optimal Control Problems with State Variable Inequality Constraints

W. E. WILLIAMSON* AND B. D. TAPLEY†
The University of Texas, Austin, Texas

A numerical method for solving optimal control problems with state variable inequality constraints (SVIC) is developed. The method is an extension of the perturbation method. The perturbation method is modified so that it can be used to solve intermediate boundary-value problems that are the results of requiring the trajectory to satisfy SVIC. An example problem, an altitude-constrained re-entry trajectory, is solved to illustrate the method. Results show that the method is a feasible method for producing numerical solutions to control problems with SVIC.

Introduction

UNFORTUNATELY, most attempts to solve realistic problems in optimal control theory require that inequality constraints that are functions of the state and/or control variables must be satisfied. The introduction of inequality constraints, particularly state variable inequality constraints (SVIC), substantially increases the problems associated with producing an optimal trajectory. In general, the application of SVIC results in a multipoint boundary-value problem instead of a two-point boundary-value problem that is associated with unconstrained optimal trajectories.

An example of a problem in which SVIC are required to produce realistic trajectories is the re-entry trajectory considered in Refs. 4 and 11. The unconstrained high-energy re-entry trajectories have unacceptable acceleration peaks and are skip trajectories. Both of these characteristics can be eliminated by requiring that the trajectory satisfy appropriate SVIC. The desire to develop a second variation technique that could be used to produce realistic optimal re-entry trajectories that satisfy the appropriate constraints provided the motivation for the method developed in this paper.

There are numerous developments of necessary conditions for SVIC in the literature. Two of these are shown in Refs. 1 and 2. Recently, new necessary conditions have been derived by Jacobson et al.[3] A penalty function approach is used which does not require the assumption of boundary segments. If the order of the constraint is greater than two, necessary conditions for an extremal which differ from those derived in Refs. 1 and 2 are obtained. For problems considered here, the order of the constraints is less than or equal to two. Hence, all of the necessary conditions in Ref. 2 agree with those given in Ref. 3.

Several numerical methods have been used to obtain solutions to optimal control problems with SVIC. Generally, these methods can be divided into penalty function methods and hard constraint methods. In the first case, a penalty term related to the constraint violation is added to the performance index. Then an attempt is made to drive the performance index to its minimum value, which in a limiting sense should drive the constraint violation to zero. The penalty function technique has been used in connection with both the gradient method[4,5] and the quasi-linearization[6] method. The hard constraint methods attempt to incorporate the constraint directly into the problem. A limiting process is not required. The direct approach has been used with both the gradient method[7] and perturbation method.[8] Comparison of penalty function techniques and hard constraint techniques using a gradient method indicates that better convergence characteristics are obtained using the hard constraint method.[7]

An alternate approach to the numerical solution of SVIC is presented by Jacobson.[9] He uses a transformation technique based on early work by Valentine to transform the SVIC into a singular arc problem. The singular arc problem is solved by a gradient method or some other method that will handle this type of problem.

If true optimal trajectories are to be calculated numerically, then a second variation method capable of incorporating the SVIC directly into the problem should be used. One method that is capable of obtaining true optimal trajectories is developed by Speyer.[10] He makes the observation that some trajectories containing SVIC are separable. This implies that parts of the trajectory not on the constraint boundary may be solved independently and pieced together with the part on the boundary. With this approach, any method, including second variation methods, may be used to obtain the segments off the boundary. However, not all problems are separable.

Reference 8 develops a linear perturbation method for solving constrained optimization problems. The method applies the necessary conditions obtained in Ref. 1. The full set of n Lagrange multipliers is used along the constraint boundary, and jumps in the values of the multipliers are considered to occur only at the time when the trajectory goes on the constraint. The method exhibits good convergence characteristics for the problems considered; however, only very simple examples are solved.

The method presented here for calculating optimal trajectories with SVIC is based on the necessary conditions given in Ref. 2. These conditions reduce the state space and hence the number of multipliers while the trajectory is on a constraint. There are no jumps in multipliers at the entry time, as in the previous two methods; however, unknown multipliers do appear at the exit boundary. A linear perturbation method is used to solve the resulting intermediate boundary-value problem.

Received December 12, 1970; revision received April 14, 1971. This work was supported by NASA under Grant NGR 44-012-178.

Index categories: Entry Vehicle Dynamics and Control; Navigation, Control, and Guidance Theory.

* Assistant Professor, Department of Aerospace Engineering and Engineering Mechanics.

† Chairman and Professor, Department of Aerospace Engineering and Engineering Mechanics.

Necessary Conditions for SVIC

The necessary conditions for SVIC summarized below are derived in Ref. 2. These conditions are obtained by dividing the optimization problem into segments that lie on the constraint boundary and segments that do not encounter the boundary. The state space is reduced for segments on the boundary, thereby implying a reduction in the number of multipliers required. Then the segments are tied together through corner conditions obtained by requiring that the first variation vanish. Only one boundary segment is considered, since necessary conditions for all boundary arcs are identical to those obtained below. The problem statement is as follows: extremize

$$I = \int_{t_0}^{t_f} Q(x,t)\, dt + \tilde{G}(x_f,t_f) \tag{1}$$

subject to $\dot{x} = f(x,u,t)$, $K(x_f,t_f) = 0$, $x(t_0) = x_{0s}$, and $S(x,t) \leq 0$, where Q and $\tilde{G}$ are scalar functions, x is an n vector of state variables, u is a scalar control, K is a q vector of terminal conditions, and x_{0s} is a specified initial state. The initial time is fixed. The constraint is a scalar function of the state and possibly the time, and its value is required to be less than or equal to zero all along the trajectory.

Following accepted notation, a pth-order constraint is defined as one for which

$$\partial/\partial u[d^kS/dt^k] = 0 \qquad k = 1,\ldots,p-1 \tag{2}$$

and

$$\partial/\partial u[d^pS/dt^p] \neq 0$$

Define

$$y^T = [S \cdots S^{p-1}] \tag{3}$$

where $S^k = d^kS/dt^k$ and y is a p vector. The vector y is a function only of x and possibly t. Note that, in order for S to be zero all along a boundary segment, it is required that $y = 0$ all along the boundary segment. Also, the control must be determined from $S^p = 0$ to force the trajectory to remain on the boundary. Thus, the number of variables required to describe the trajectory along a boundary arc is reduced from n to $(n-p)$. Choose $(n-p)$ state variables, Z, to describe the trajectory along the constraint. In general, the Z's will be chosen as $(n-p)$ of the original state variables x, which are not affected by the constraint. Thus,

$$Z^T = [Z_1(x,t)\cdots Z_{(n-p)}(x,t)] \tag{4}$$

and the Z's are chosen such that

$$|(\partial y/\partial x)/(\partial Z/\partial x)| \neq 0 \tag{5}$$

The last condition allows x to be determined as a function of y and Z.

The optimization problem can then be divided into arcs on the boundary and arcs off the boundary. On the boundary, the state is determined from the conditions

$$\dot{Z} = g(Z,t) \qquad y = 0 \tag{6}$$

where $g(Z,t)$ is the $(n-p)$ vector of derivatives of the Z variables along the constraint boundary. The control is eliminated from the Z equations by using $S^p = 0$.

The necessary conditions for an extremal with a boundary segment are thus: at the initial time,

$$t = 0 \qquad x(t_0) = x_{0s} \tag{7}$$

At the final time,

$$K = 0 \qquad \lambda(t_f) = P_{x_f}{}^T \qquad H + P_{t_f} = 0 \tag{8}$$

On unconstrained arcs,

$$\dot{x} = H_\lambda{}^T \qquad \dot{\lambda} = -H_x{}^T \qquad H_u = 0 \tag{9}$$

On constrained arcs,

$$\dot{Z} = G_\mu{}^T \qquad \dot{\mu} = -G_Z{}^T \qquad y = 0 \qquad S^p = 0 \tag{10}$$

And at each junction point,

$$H - G + \lambda^T(My_t + NZ_t) = 0 \qquad \mu^T - \lambda^TN = 0 \qquad y = 0 \qquad Z = Z(x,t) \tag{11}$$

where the matrices M and N are defined as

$$[M|N] = [y_x/Z_x]^{-1} \tag{12}$$

M is an $n \times p$ matrix, and N is an $n \times (n-p)$ matrix. λ is the n vector of multipliers associated with the x's, and μ is the $n-p$ vector of multipliers associated with the Z's. The variational Hamiltonian off of the boundary is $H = \lambda^Tf + Q$. On the boundary, the Hamiltonian is $G = \mu^Tg + Q$, where Q is evaluated along $y = 0$. Also, $P = \tilde{G} + \nu^TK(x_f, t_f)$, where ν is a q vector of multipliers. Note that, as a boundary segment is entered, the multipliers μ are uniquely determined from the second equation in Eq. (11). As the boundary is left, p of the λ's cannot be determined directly from these boundary conditions. Note that, in general, an unconstrained optimal trajectory is characterized as a two-point boundary-value problem. Here necessary conditions for an optimal trajectory with a SVIC are formulated as a multipoint boundary-value problem. Modifications to the standard MPF (method of perturbation functions[12]) to include these additional conditions are considered in the next section.

Application of Perturbation Method to SVIC

A perturbation method now will be derived to solve the intermediate boundary-value problem described by Eqs. (7–11). Again this will be derived for only one SVIC boundary segment. The extension to more than one segment is straightforward.

Off the constraint boundary, the control is eliminated from the problem formulation by using the conditions $H_u = 0$ and $H_{uu} \geq 0$. Thus, off the boundary the optimal trajectory is defined by a system of $2n$ first-order differential equations consisting of the first two equations in Eq. (9). On the boundary, the trajectory is defined by the $2(n-p)$ system of equations shown as the first two equations in Eq. (10). Thus, the problem has been reduced to an intermediate boundary-value problem.

Corresponding to the standard MPF method, unknown multipliers and unknown boundary times will be guessed. At the boundary exit, either p of the λ's or all of the λ's may be guessed. If all of the λ's are guessed, the equation relating λ's and μ's may be considered as boundary conditions to be satisfied by the iteration procedure. The latter procedure will be followed here. For the second example, the other procedure will be used. The initial multipliers, multipliers at the boundary exit, the boundary entry time, boundary exit time, and final time will all be guessed. A nominal trajectory is produced by integrating the $\dot{x}$ and $\dot{\lambda}$ equations from t_0 to t_1 using specified values for x_0 and guessed values for λ_0. At t_1, Z and μ are determined from $Z = Z(x,t)$ and $\mu^T = \lambda^TN$. The equations for $\dot{Z}$ and $\dot{\mu}$ are integrated from t_1 to t_2. At t_2, x is determined from $Z = Z(x,t)$ and $y = 0$. The values of λ at t_2 are guessed, and the $\dot{x}$ and $\dot{\lambda}$ equations are integrated from t_2 to t_f. Changes in the guessed variables are then related to desired changes in the unsatisfied boundary conditions using linear perturbation theory. Corrections to the guessed variables λ_0, λ_2, t_1, t_2, and t_f are calculated to drive all of the unsatisfied boundary conditions to zero. This procedure is continued until the values of the conditions are sufficiently small. Boundary conditions that will not be satisfied by the nominal are given below.

At the boundary entry time, $Z = Z(x,t)$ determines Z, and $\mu^T = \lambda^TN$ determines μ. The $(p+1)$ unsatisfied boundary

conditions for the nominal trajectory are

$$h_1 = \begin{bmatrix} H - G + \lambda^T(My_t + NZ_t) \\ y \end{bmatrix}_{t_1} \tag{13}$$

At the exit time, $Z = Z(x,t)$ and $y(x,t) = 0$ determine x at t_2. This leaves $(n - p + 1)$ unsatisfied boundary conditions:

$$h_2 = \begin{bmatrix} H - G + \lambda^T(My_t + NZ_t) \\ \mu^T - \lambda^T N \end{bmatrix}_{t_2} \tag{14}$$

At the final time, the usual $(n + 1)$ unconstrained boundary conditions are still applicable and are expressed as

$$h_f(x_f,\lambda_f,t_f) = 0 \tag{15}$$

where the ν vector has been eliminated from Eq. (8). This gives $(2n + 3)$ unsatisfied boundary conditions and $(2n + 3)$ unknowns, which are $\lambda(t_0)$, $\lambda(t_2)$, t_1, t_2, and t_f. Corrections in these quantities are now related to desired changes in boundary conditions. Define

$$z^T = [x^T : \lambda^T] \qquad v^T = [z^T : \mu^T] \tag{16}$$

and then

$$\delta z_1 = \Phi(1,0)\delta z_0 \qquad \delta v_2 = \Phi(2,1)\delta v_1$$
$$\delta z_f = \Phi(f,2)\delta z_2 \tag{17}$$

where $\Phi(1,0)$ and $\Phi(f,2)$ are $2n \times 2n$ transition matrices and $\Phi(2,1)$ is a $2(n - p) \times 2(n - p)$ transition matrix. Here $\Phi(a,b)$ denotes the solution of the appropriate set of linear perturbation equations, which have been integrated from t_b to t_a, with the initial conditions at t_b set equal to the identity matrix.

Note that, at a boundary, v is an explicit function of x and λ. Then

$$\Delta v = (\partial v/\partial z)\ \Delta z + (\partial v/\partial t)\ \Delta t \tag{18}$$

Also, $\Delta z = \delta z + \dot{z}\Delta t$ at the boundaries.

The boundary conditions are expanded about the nominal and then related to the assumed values of the unknown boundary condition. For the conditions at t_1,

$$\Delta h_1 = (\partial h_1/\partial z_1)\ \delta z_1 + \dot{h}_1 \Delta t_1 \tag{19}$$

Using the Φ matrix,

$$\Delta h_1 = (\partial h_1/\partial z_1)\Phi(1,0)\delta z_0 + \dot{h}_1 \Delta t_1 \tag{20}$$

Since the initial state is fixed, $\delta z_0{}^T = [0^T : \delta\lambda_0{}^T]$. Then only the last n columns of the $\Phi(1,0)$ matrix are required, and

$$\Delta h_1 = (\partial h_1/\partial z_1)\Phi_2(1,0)\delta\lambda_0 + \dot{h}_1 \Delta t_1 \tag{21}$$

where $\Phi_2(1,0)$ is the last n columns of the $\Phi(1,0)$ matrix. Similarly, for t_2,

$$\Delta h_2 = (\partial h_2/\partial v_2)\Delta v_2 + (\partial h_2/\partial \lambda_2)\ \Delta\lambda_2 + (\partial h_2/\partial t_2)\ \Delta t_2 \tag{22}$$

where the corrections to $\lambda(t_2)$ are separated from other terms at t_2, since corrections to $\lambda(t_2)$ must be calculated.

Since $\Delta v_2 = \delta v_2 + \dot{v}_2 \Delta t_2$ and $\delta v_2 = \Phi(2,1)\delta v_1$, then

$$\Delta h_2 = (\partial h_2/\partial v_2)\Phi(2,1)\ \delta v_1 + (\partial h_2/\partial \lambda_2)\ \Delta\lambda_2 + [(\partial h_2/\partial t_2) + (\partial h_2/\partial v_2)\dot{v}_2]\ \Delta t_2 \tag{23}$$

Again, $\delta v_1 = \Delta v_1 - \dot{v}_1 \Delta t_1$ and $\Delta v_1 = (\partial v_1/\partial z_1)\ \Delta z_1 + (\partial v_1/\partial t_1)\ \Delta t_1$, so that

$$\Delta h_2 = (\partial h_2/\partial \lambda_2)\ \Delta\lambda_2 + (\partial h_2/\partial v_2)\Phi(2,1) \times (\partial v_1/\partial z_1)\Phi_2(1,0)\ \delta\lambda_0 - (\partial h_2/\partial v_2)\Phi(2,1)[\dot{v}_1 - (\partial v_1/\partial t_1) - (\partial v_1/\partial z_1)\dot{z}_1]\ \Delta t_1 + [(\partial h_2/\partial t_2) + (\partial h_2/\partial v_2)\dot{v}_2]\ \Delta t_2 \tag{24}$$

Note that total changes $\Delta\lambda_2$ are calculated for the multipliers at t_2 and that changes in h_2 are linearly related to changes in $\lambda(t_0)$,$\lambda(t_2)$, t_1, and t_2.

For the final time,

$$\Delta h_f = (\partial h_f/\partial z_f)\delta z_f + \dot{h}_f \Delta t_f \tag{25a}$$

$$\Delta h_f = (\partial h_f/\partial z_f)\Phi(f,2)\delta z_2 + \dot{h}_f \Delta t_f \tag{25b}$$

or

Define $(\partial h_f/\partial z_f)\Phi(f,2) = [\bar{\Phi}_1(f,2)|\bar{\Phi}_2(f,2)]$, where $\bar{\Phi}_1$ and $\bar{\Phi}_2$ are $(n + 1) \times n$ matrices. Then

$$\Delta h_f = \bar{\Phi}_1(f,2)\ \delta x_2 + \bar{\Phi}_2(f,2)\ \delta\lambda_2 + \dot{h}_f \Delta t_f \tag{26a}$$

or

$$\Delta h_f = \bar{\Phi}_1(f,2)\ \Delta x_2 + \bar{\Phi}_2(f,2)\ \Delta\lambda_2 - [\bar{\Phi}_1(f,2)\dot{x}_2 + \bar{\Phi}_2(f,2)\dot{\lambda}_2]\ \Delta t_2 + \dot{h}_f \Delta t_f \tag{26b}$$

Changes in x are related to changes in z by

$$\Delta x_2 = (-My_t - NZ_t)|_{t_2}\Delta t_2 + N_2 \Delta Z_2 \tag{27}$$

Define $\bar{N}_2$ such that

$$N_2 \Delta Z_2 = \bar{N}_2 \Delta v_2 \qquad \text{or} \qquad \bar{N}_2 = [N_2|0] \tag{28}$$

$\bar{N}_2$ is an $n \times 2(n - p)$ matrix. Then

$$\Delta h_f = \bar{\Phi}_1(f,2)\bar{N}_2\delta v_2 + \bar{\Phi}_2(f,2)\ \Delta\lambda_2 - [\bar{\Phi}_1(f,2)\dot{x}_2 + \bar{\Phi}_2(f,2)\dot{\lambda}_2 - \bar{\Phi}_1(f,2)(\bar{N}_2\dot{v}_2 + My_t + NZ_t)]\ \Delta t_2 + \dot{h}_f \Delta t_f \tag{29}$$

and

$$\Delta h_f = \bar{\Phi}_2(f,2)\Delta\lambda_2 + \bar{\Phi}_1(f,2)\bar{N}_2\Phi(2,1)(\partial v_1/\partial z_1)\Phi_2(1,0)\ \delta\lambda_0 + \{\bar{\Phi}_1(f,2)\bar{N}_2\Phi(2,1)[\dot{v}_1 - (\partial v_1/\partial t_1) - (\partial v_1/\partial z_1)\dot{z}_1]\}\ \Delta t_1 - \{\bar{\Phi}_1(f,2)\dot{x}_2 + \bar{\Phi}_2(f,2)\dot{\lambda}_2 - \bar{\Phi}_1(f,2)\bar{N}\dot{v}_2 + My_t + NZ_t\}\ \Delta t_2 + \dot{h}_f \Delta t_f \tag{30}$$

The three vector equations, Eqs. (21, 24, and 30), must be solved simultaneously for the corrections to the assumed values of the unknown quantities. These corrections are added to the assumed values of the variables, and the iteration procedure is continued until the value of each h is sufficiently small.

The entire fundamental matrix must be integrated from t_1 to t_2 and from t_2 to t_f. Thus, the integration of a large number of variables is required for constrained trajectories.

The major disadvantage of this method is the necessity of guessing the number of boundary arcs and their approximate location. For many problems, however, unconstrained optimal trajectories may be obtained. These unconstrained trajectories provide insight into the location of boundary segments. They also provide reasonable estimates for boundary entry and exit times. If some information about the location of boundary arcs is available, the convergence characteristics of the method, presented in the previous discussion, indicate that it is a feasible method for attacking problems with SVIC.

In order to check out the method described earlier, it was used first to calculate the optimal solution to the constrained Brachistochrone problem discussed in Refs. 1 and 6. The complete results of this study are shown in Ref. 12. The method was found to be quite easy to implement for this example. The method also exhibited good convergence characteristics for this example. That is, only a reasonably small number of iterations were required to produce converged trajectories for several initial guesses for the unknown variables.

Altitude-Constrained Re-Entry

The second example considered is the application of an altitude constraint to an Apollo-type re-entry trajectory for

a lunar return mission.

The state equations are

$$\begin{aligned} \dot{r} &= V\sin\gamma \qquad \dot{\theta} = V\cos\gamma\cos\psi/(r\cos\phi) \\ \dot{\phi} &= V\cos\gamma\sin\psi/r \qquad \dot{V} = \mu\sin\gamma/r^2 - D \\ \dot{\gamma} &= [-\mu/(r^2V) + V/r]\cos\gamma + L\cos\beta/V \\ \dot{\psi} &= -V\cos\gamma\cos\psi\tan\phi/r - L\sin\beta/(V\cos\gamma) \end{aligned} \tag{31}$$

where r is the distance from the center of the earth to the center of mass of the vehicle, θ is the longitude, ϕ is the latitude, V is the magnitude of the velocity, γ is the flight path angle, ψ is the heading angle, L and D are the lift and drag per unit mass, μ is the gravitational constant, and β is the roll angle of the vehicle (the control). For the Apollo vehicle, the lift coefficient, C_L, and the drag coefficient C_D are assumed to be constant. An exponential model is used for the atmosphere.

Since the two main problems associated with re-entry are the acceleration and heating, the performance index is chosen as a linear sum of the integral of the acceleration and the integral of the convective heating rate. Here

$$I = \int_{t_0}^{t_f} [\tfrac{1}{2}(C_L^2 + C_D^2)^{1/2}S^*\rho V^2 + \lambda_c\rho^{1/2}V^3]\,dt \tag{32}$$

where S^* is the reference area of the vehicle per unit mass, ρ is the density of the atmosphere, and λ_c is the numerical constant associated with the convective heating rate times a weighting constant. In this study, λ_c is chosen to give approximately equal weighting to the acceleration and convective heating terms.

Boundary conditions consist of a specified initial state and time. Final values of θ, ϕ, and V are specified, and t_f is free. A complete description of the re-entry problem considered here may be found in Refs. 12 and 13. Unconstrained optimal re-entry trajectories are shown in both references. Optimal trajectories produced there are skip trajectories with high peak accelerations. Since optimal trajectories that remain in the sensible atmosphere are desired for Apollo missions, an altitude constraint is applied to trajectory. The SVIC is thus

$$S(x,t) = r - r_d \leq 0 \tag{33}$$

where r_d denotes a specified altitude. Since the initial altitude r_0 will be larger than r_d, the constraint applies only after the re-entry altitude becomes less than or equal to the constraint altitude. This is a second-order constraint, as seen from taking derivatives of S:

$$\dot{S} = \dot{h} = V\sin\gamma = 0 \tag{34}$$

implying $\gamma = 0$. Also,

$$\ddot{S} = \ddot{h} = \dot{V}\sin\gamma + (V\cos\gamma)\dot{\gamma} = 0 \tag{35}$$

implying $\dot{\gamma} = 0$, or

$$\begin{aligned} \cos\beta &= [\mu/(r_d^2V^2) - 1/r_d]/(S^*C_L\rho_d/2) \\ \sin\beta &= (1 - \cos^2\beta)^{1/2} \end{aligned} \tag{36}$$

The plus sign has been chosen for $\sin\beta$, since, for this study, only negative values of ϕ are considered. It would seem reasonable to have the vehicle roll in the direction of the desired terminal value of ϕ, which in this case implies that $\sin\beta$ should be positive.

On the altitude constraint, the Z variables are chosen as θ, ϕ, V, and ψ. This is the natural choice for the Z variables, since this choice gives a one-to-one correspondence between the μ vector and four variables in the λ vector. The equations for $\dot{Z}$ are thus

$$\begin{aligned} \dot{\theta} &= VC\psi/(r_dC\phi) \qquad \dot{\phi} = VS\psi/r_d \\ \dot{V} &= -(\tfrac{1}{2}S^*C_D)\rho_dV^2 \\ \dot{\psi} &= -VC\psi\tan\phi/r_d - (\tfrac{1}{2}S^*C_L)\rho_dVS\beta \end{aligned} \tag{37}$$

where $\cos\psi = C\psi$, $\sin\psi = S\psi$, . . . , have been used. The y equations are

$$y_1 = r - r_d = 0 \qquad y_2 = \gamma = 0 \tag{38}$$

Boundary conditions at entering and exiting times require continuity of the state variables, and also

$$\begin{gathered} \mu_\theta = \lambda_\theta \qquad \mu_\phi = \lambda_\phi \qquad \mu_V = \lambda_V \qquad \mu_\psi = \lambda_\psi \\ G = H \qquad r - r_d = 0 \qquad \gamma = 0 \end{gathered} \tag{39}$$

Additional conditions that must be satisfied at the final time are

$$\begin{gathered} \lambda_r(t_f) = 0 \qquad \lambda_\gamma(t_f) = 0 \qquad \lambda_\psi(t_f) = 0 \\ H(t_f) = 0 \end{gathered} \tag{40}$$

Differential equations for the λ's, μ's, and the perturbation equations are shown in Ref. 12. The reduction to the intermediate boundary-value problem is shown there also.

A nominal trajectory must be produced first. Again one boundary arc is assumed. The first four conditions of Eq. (39) can be satisfied on every integration. At t_1, the values of μ are set equal to the numerically integrated values of $\lambda(t_1)$. At t_2, four of the λ's are set equal to the numerically integrated values of $\mu(t_2)$. Thus only two of the λ variables, λ_r and λ_γ, must be guessed at t_2. Also, at t_2, the integration of the x equations is begun with $r = r_d$ and $\gamma = 0$. Hence the only intermediate boundary conditions that cannot be satisfied on every iteration are

$$\begin{aligned} &\text{at } t_1 \qquad G = H \qquad r - r_d = 0 \qquad \gamma = 0 \\ &\text{at } t_2 \qquad G = H \end{aligned} \tag{41}$$

Unknowns associated with the problem include the initial values of λ (six variables), λ_r and λ_γ at t_2 (two variables), and the times t_1, t_2, and t_f. Thus there are 11 unknowns. Boundary conditions consist of the seven original terminal conditions for the unconstrained problem and the four conditions just shown, or a total of 11 boundary conditions. The number of boundary conditions is thus equal to the number of unknowns, and a well-posed problem exists.

For the numerical calculations, conditions on the Hamiltonian are applied in a different manner. Since the Hamiltonian is constant along the entire trajectory, it is required to be zero initially, i.e., $H(t_0) = 0$. This condition replaces the last condition in Eq. (40). The continuous Hamiltonian at the entry and exit boundary times requires that the control be continuous at the boundaries. This condition may be expressed as

$$[\mu/(r_dV^2) - 1](\lambda_\psi^2 + \lambda_\gamma^2)^{1/2}/(S^*C_Lr_d\rho_d/2) + \lambda_\gamma = 0 \tag{42}$$

All necessary conditions on the Hamiltonian will be satisfied if these three conditions are satisfied.

For this problem, all of the multipliers at the exit time are not guessed. In order to decrease the dimensionality of the linear system to be solved, only the two multipliers λ_r and λ_γ are guessed. The theory developed in the previous section must be altered slightly to include this change. The effects of $\Delta\lambda_r(t_2)$ and $\Delta\lambda_\gamma(t_2)$ are separated out, and changes in the other λ's at t_2 are linearly related to changes in μ at t_2. If the two-vector

$$\lambda_u{}^T = [\lambda_r|\,\lambda_\gamma]_{t_2} \tag{43}$$

is defined, then the linear equations for h with y_t and Z_t equal to zero are

$$\Delta h_0 = (\partial h_0/\partial\lambda_0)\,\delta\lambda_0 \tag{44}$$

$$\Delta h_1 = (\partial h_1/\partial z_1)\Phi_2(1,0)\,\delta\lambda_0 + \dot{h}_1\Delta t_1 \tag{45}$$

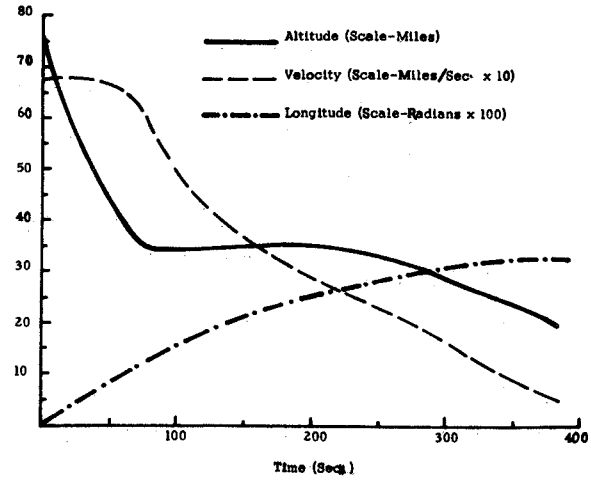

Fig. 1 State variables r, θ, and V for optimal, constrained re-entry.

$$\Delta h_2 = (\partial h_2/\partial \lambda_u)\,\Delta\lambda_u + (\partial h_2/\partial v_2)\Phi(2,1)(\partial v_1/\partial z_1)\Phi_2(1,0) \times \delta\lambda_0 + (\partial h_2/\partial v_2)\Phi(2,1)[(\partial v_1/\partial z_1)\dot{z}_1 - \dot{v}_1]\,\Delta t_1 + (\partial h_2/\partial v_2)\dot{v}_2\Delta t_2 \quad (46)$$

$$\Delta h_f = \bar{\Phi}(f,2)\,\Delta\lambda_u + \bar{\Phi}(f,2)\Phi(2,1)(\partial v_1/\partial z_1)\Phi_2(1,0)\,\delta\lambda_0 + \bar{\Phi}(f,2)\Phi(2,1)[\partial v_1/\partial z_1\dot{z}_1 - \dot{v}_1]\,\Delta t_1 + [\bar{\Phi}(f,2)\dot{v}_2 - \partial h_f/\partial z_f\Phi(2,1)\dot{z}_2]\,\Delta t_2 + \dot{h}_f\Delta t_f \quad (47)$$

where

$$\bar{\Phi}(f,2) = \partial h_f/\partial z_f\Phi(f,2)B_1 \quad (48)$$

and

$$B_1{}^T = \left[\begin{array}{cccccc:cccccc} 0 & 1 & 0 & 0 & 0 & 0 & & & & & & \\ 0 & 0 & 1 & 0 & 0 & 0 & & & 0 & & & \\ 0 & 0 & 0 & 1 & 0 & 0 & & & & & & \\ 0 & 0 & 0 & 0 & 0 & 1 & & & & & & \\ \hdashline & & & & & & 0 & 1 & 0 & 0 & 0 & 0 \\ & & & 0 & & & 0 & 0 & 1 & 0 & 0 & 0 \\ & & & & & & 0 & 0 & 0 & 1 & 0 & 0 \\ & & & & & & 0 & 0 & 0 & 0 & 0 & 1 \end{array}\right]$$

B_1 is a 12×8 matrix, and $\bar{\Phi}(f,2)$ is a 6×8 matrix. Also,

$$\bar{\Phi}(f,2) = (\partial h_f/\partial z_f)\Phi(f,2)B_2 \quad (49)$$

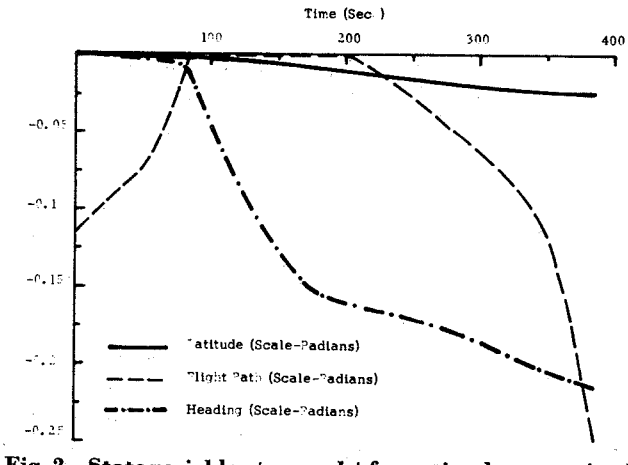

Fig. 2 State variables ϕ, γ, and ψ for optimal, constrained-re-entry trajectory.

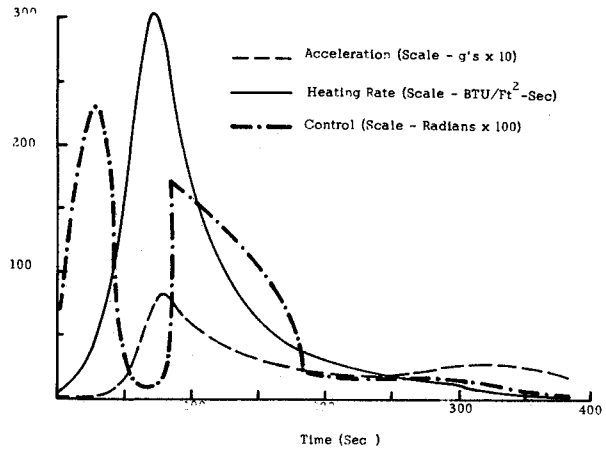

Fig. 3 Control, acceleration, and heating rate for optimal re-entry trajectory.

where

$$B_2{}^T = \begin{bmatrix} 0 & 0 & 0 & 0 & 0 & 0 & 1 & 0 & 0 & 0 & 0 & 0 \\ 0 & 0 & 0 & 0 & 0 & 0 & 0 & 0 & 0 & 0 & 1 & 0 \end{bmatrix}$$

B_2 is a 12×2 matrix, and $\bar{\Phi}(f,2)$ is a 6×2 matrix.

Thus, $\bar{\Phi}(f,2)$ separates out the coefficients for $\Delta\lambda_u$, and $\bar{\Phi}(f,2)$ includes the other terms after realizing that Δr_2 and $\Delta\gamma_2$ are zero. All other terms correspond directly to the previous development.

The numerical values for the initial conditions are $r_0 = 4035.758$ miles (400,000 ft), $\theta_0 = 0.0$ rad, $\phi_0 = 0.0$ rad, $V_0 = 6.8181818$ miles/sec (36,000 fps), $\gamma_0 = 0.1134464$ rad ($-6.5°$), and $\psi_0 = 0.0$ rad. The terminal conditions are $\theta_{fs} = 0.33$ rad, $\phi_{fs} = -0.025$ rad, and $V_{fs} = 0.5$ miles/sec.

The initial multipliers for the unconstrained trajectory shown in Ref. 12 will be used as initial multipliers for the iteration procedure here. These values, guesses for the unknown vector λ_u, and guesses for t_1, t_2, and t_f are shown in Table 1. The constraint altitude chosen is $r_d = 3995.0$ miles. The same numerical integrator discussed earlier is used here.

Approximately 32 sec of computer time on the CDC 6600 is required for each iteration of the constrained re-entry trajectory. The method requires 104 iterations to converge. Plots of the states, control, acceleration, and heating rate are shown in Figs. 1–3.

The modified MPF does very well for the first few iterations, and then the norm begins to decrease very slowly for a considerable number of iterations. Over this interval, the signs on the corrections of most of the variables oscillate back and forth from plus to minus. Elements of the linear system produced by the transition matrices change only in about the third or fourth digits. The flight-path angle at t_f over this interval is near $-60°$. It is changing very rapidly near the end of the trajectory, and, if the equations are integrated for a few more seconds past the nominal final time, it quickly approaches $-90°$. A singularity exists in the equations at $-90°$, and accurate integration near this singularity is very difficult. The iteration continues for about 70 iterations, slowly increasing γ. After the flight-path angle is changed to $-35°$, the method begins to converge very rapidly again.

Another problem is that large corrections oscillating from plus to minus are calculated at t_2. The control along the boundary segment is calculated from Eq. (36). If the time calculated for t_2 is sufficiently large, the velocity along the boundary becomes small enough to make the absolute value of $\cos\beta$ greater than one. This indicates that the vehicle cannot fly at a specified altitude for an infinite time interval. If the value of t_2 is larger than the maximum time interval

Table 1 Nominal and converged multipliers for constrained re-entry

Variable	Nominal value	Converged value
λ_{r_0}	−1.26588E-3	−1.2772884E-2
λ_{θ_0}	−9.181666	−7.40988123
λ_{ϕ_0}	26.5966	3.3857227
λ_{V_0}	2.35619	3.15221059
λ_{γ_0}	13.82719	−1.20936003
λ_{ψ_0}	8.84954	9.63840795E-1
λ_{r_2}	1.0E-2	5.33051908E-3
λ_{γ_2}	−1.0E-1	−8.16314647E-1
t_1	70.0	85.0966654
t_2	150.0	184.938154
t_f	320.0	383.410663

that the vehicle can remain on the boundary, then $\sin\beta$ becomes imaginary.

For the preceding iterations, the nominal value of t_2 approaches this value after 30 iterations. From this point on, if large positive corrections are accepted for t_2 an imaginary value of $\sin\beta$ is obtained. Thus, even though corrections to t_2 are oscillating from plus to minus, allowing fairly large corrections (7.0 sec) results in nominal trajectories that require imaginary control. Requiring small corrections for t_2 and hence the rest of the correction vector slows down the convergence process and is partially responsible for the large number of iterations required for convergence.

These two problems also affect convergence for other nearby optimal trajectories. When the flight-path angle begins to change rapidly and approach −90°, iteration problems are encountered. For example, a nearby optimal characterized by r_d = 3995.3 miles and θ_{fs} = 0.34 rad is computed. The converged values shown in Table 1 are used as initial guesses for the unknown variables. The trajectory produced after the third iteration integrates through the singularity (γ = −90°) near the end of the trajectory. The method diverges at this point. If the converged values shown in Table 1 are used and the final time t_f is changed to 360.0 sec, the method converges to the new optimal in 17 iterations. Changing the guess for t_f from 383.4 to 360.0 sec allows the method to iterate without encountering the singularity. Thus, nearby optimal trajectories can be produced with a relatively few number of iterations if the singularity is avoided.

It is believed that integration accuracy and hence convergence characteristics would be improved by regularizing the nonlinear re-entry equations, Eqs. (31). This is done for unconstrained trajectories calculated in Refs. 11 and 12, when similar problems are encountered. Results from that study indicate that regularization does improve convergence in some cases.

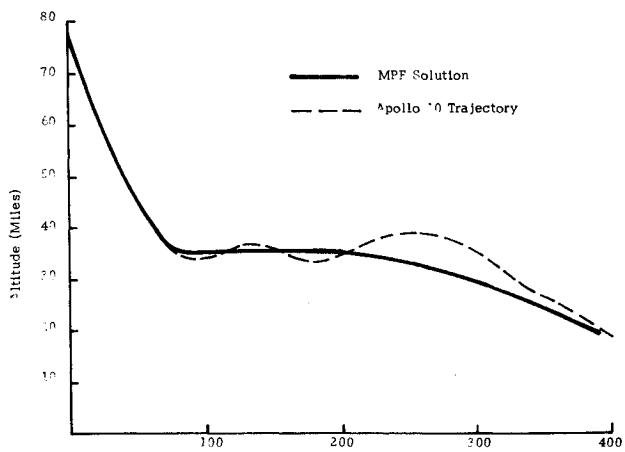

Fig. 4 Comparison of altitude histories for constrained optimal trajectory and Apollo 10 trajectory.

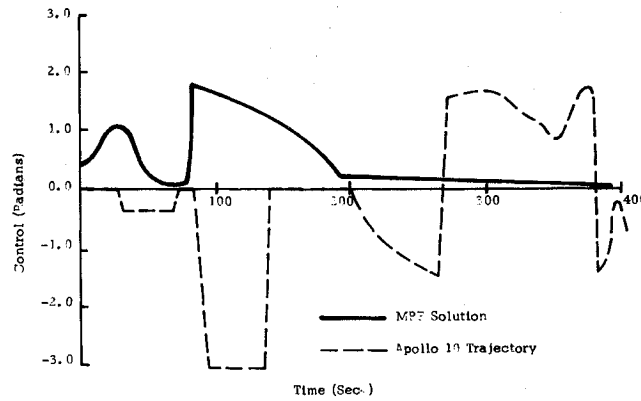

Fig. 5 Comparison of control programs for constrained optimal trajectory and Apollo 10 trajectory.

Trajectories obtained with the altitude SVIC represent realistic re-entry trajectories. The maximum acceleration peak is 8.3 g's, and over most of the trajectory the acceleration is 2 or 3 g's. The maximum heating rate for the trajectory is 306.8 Btu/ft²-sec, and the total heat absorbed is 24013.2 Btu/ft². These heating data are calculated using the equation

$$Q_c = 1.1(17600/6.4167^{0.5})(\rho/0.0023769)^{0.5}(V/26000)^{3.15} \quad \text{Btu/(ft}^2\text{-sec)} \quad (50)$$

The method used to generate solutions to problems with SVIC in this report can produce solutions that violate the constraint. If the values of the terminal conditions are not consistent with the inequality constraint, trajectories that remain on the constraint for a short segment and then violate the constraint may be produced. For instance, the altitude constraint limits the range capabilities of the vehicle. If values of θ_{fs} and ϕ_{fs} are specified which cannot be reached if the vehicle remains below the altitude constraint, the method will converge to a trajectory with a short segment on the boundary. After the boundary segment, the vehicle will roll the lift vector upward and penetrate the constraint in order to satisfy the boundary conditions. The method does converge, however, and the solution obtained does give the user a trajectory with, in general, a small constraint violation. From observing the trajectory, it will usually be apparent that the terminal conditions and constraint are inconsistent. The converged trajectory gives good estimates of variables to be used for a consistent set of conditions.

Plots of the altitude, control, and acceleration for the Apollo 10 trajectory are shown in Ref. 13. These graphs

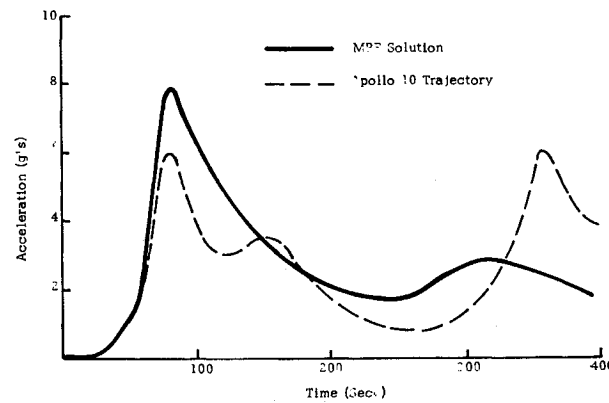

Fig. 6 Comparison of acceleration histories for constrained optimal trajectory and Apollo 10 trajectory.

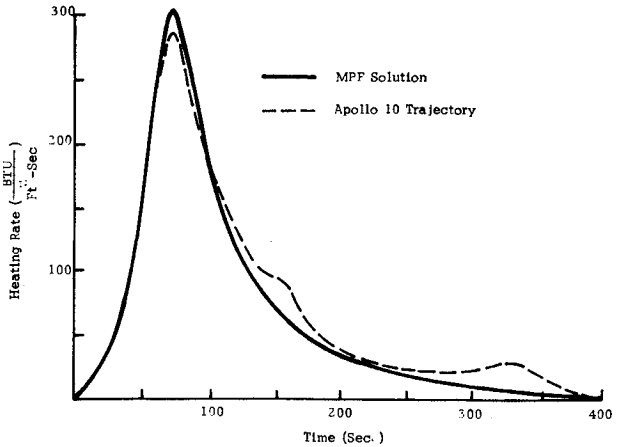

Fig. 7 Comparison of convective heating rate histories for constrained optimal trajectory and Apollo 10 trajectory.

are compared with the same plots for the optimal constrained trajectory computed with $r_d = 3995.3$ miles, $\theta_{fs} = 0.34$ rad, $\phi_{fs} = -0.025$ rad, and $V_{fs} - 0.5$ miles/sec in Figs. 4–7. The two trajectories are quite similar. The Apollo vehicle rolls both to the right and to the left in an attempt to land in approximately the same plane as the one it is in when it begins to re-enter the atmosphere. The calculated optimal trajectories roll only in one direction and hence land out of the initial flight plane, in this case by -0.025 rad.

The other difference in the two trajectories is the short skip segment at $t = 260$ sec for the Apollo trajectory. This skip is responsible for the small acceleration near the peak of the skip and also for the high acceleration as the vehicle flies back into the dense atmosphere. Trajectories that have the small skip segment in this location are obtained by the modified MPF if a final value of θ_{fs} is specified which cannot be reached by the vehicle if it remains below the altitude constraint.

The total heating for the optimal trajectory is 25,561 Btu/ft², whereas the heating listed for the Apollo trajectory is 26,000 Btu/ft². Hence, the performance index chosen here permits slightly higher peak accelerations than the Apollo 10 trajectory but decreases slightly the total heat absorbed. The results of this comparison show that the choice of the performance index used here and the inclusion of the altitude constraint can be used to generate realistic optimal re-entry trajectories.

Summary

The perturbation method has been modified to solve optimal control problems involving state variable inequality constraints. Two example problems, constrained Brachistochrone and an altitude-constrained re-entry trajectory, are solved. The number of iterations required to converge trajectories is shown to be reasonable in all cases where singularities in the differential equations are not encountered. The results obtained for the Apollo re-entry problem are shown to be realistic optimal trajectories.

References

[1] Bryson, A. E., Denham, W. F., and Dreyfus, S. E., "Optimal Programming Problems with Inequality Constraints I: Necessary Conditions for Extremal Solutions," *AIAA Journal*, Vol. 1, No. 11, Nov. 1963, pp. 2544–2551.

[2] Speyer, J. L. and Bryson, A. E., Jr., "Optimal Programming Problems with a Bounded State Space," *AIAA Journal*, Vol. 6, No. 8, Aug. 1968, pp. 1488–1491.

[3] Jacobson, D. H., Lele, M. M., and Speyer, J. L., "New Necessary Conditions of Optimality for Control Problems with State-Variable Inequality Constraints," to be published.

[4] Wagner, W. E. and Jazwinski, A. H., "Three-Dimensional Reentry Optimization with Inequality Constraints," AIAA Paper 63-419, New Haven, Conn., 1963.

[5] Kelley, H. J., "Method of Gradients," *Optimization Techniques*, edited by G. Leitmann, Academic Press, New York, 1962, Chap. 6, p. 230.

[6] McGill, R., "Optimal Control, Inequality State Constraints, and the Generalized Newton-Raphson Algorithm," *SIAM Journal on Control*, Vol. 3, No. 2, 1965, pp. 291–298.

[7] Denham, W. F. and Bryson, A. E., "Optimal Programming Problems with Inequality Constraints II: Solution by Steepest-Ascent," *AIAA Journal*, Vol. 2, No. 1, Jan. 1964, pp. 25–34.

[8] Hamilton, W. E. and Koivo, A. J., "On Computational Solutions of State Constrained Optimization Problems," *Proceedings of the Joint Automatic Control Conference*, American Automatic Control Council, Aug. 1969, p. 384.

[9] Jacobson, D. H. and Lele, M. M., "A Transformation Technique for Optimal Control Problems with a State Variable Inequality Constraint," TR 574, 1968, Div. Engineering and Applied Physics, Harvard Univ., Cambridge, Mass.

[10] Speyer, J. L., Mehra, R. K., and Bryson, A. E., Jr., "The Separate Computation of Arcs for Optimal Flight Paths with State Variable Inequality Constraints," TR 526, May 1967, Div. of Engineering and Applied Physics, Harvard Univ., Cambridge, Mass.

[11] Tapley, B. D., Fowler, W. T., and Williamson, W. E., "The Computation of Optimal Apollo-Type Reentry Trajectories," *Proceedings of the Joint Automatic Control Conference*, American Automatic Control Council, Aug. 1969, p. 281.

[12] Williamson, W. E., "Optimal Three Dimensional Reentry Trajectories for Apollo Type Vehicles," EMRL Rept. 1013, 1970, The Univ. of Texas at Austin, Austin, Texas.

[13] "Spacecraft Operational Trajectory for Apollo Mission F, Volume I—Operational Mission Profile Launched May 17, 1969," Internal Note 69-FM-65, March 26, 1969, George C. Marshall Space Flight Center, Huntsville, Ala.